PHYSICAL REVIEW D **81,** 051501(R) (2010)

QCD motivated approach to soft interactions at high energy: Inclusive production

E. Gotsman, E. Levin, and U. Maor

Department of Particle Physics, School of Physics and Astronomy, Raymond and Beverly Sackler Faculty of Exact Science, Tel Aviv University, Tel Aviv 69978, Israel

(Received 1 February 2010; published 10 March 2010)

We extend our two-component Pomeron, Gotsman-Levin-Maor-Miller (GLMM) model, for soft high-energy scattering to single inclusive cross sections. To this end we present a suitable formulation which also includes the semienhanced Pomeron-particle vertex corrections. The available data on single inclusive density $(1/\sigma_{\rm in})d\sigma/dy$ in the c.m. energy range of 200–1800 GeV are well reproduced by our model. The just-published ALICE Collaboration point at 900 GeV is in excellent agreement with the calculations of our model. We also present predictions covering the complete LHC energy range which can be readily tested in the early low-luminosity LHC runs. The results presented in this paper provide additional support to our Pomeron model approach.

DOI: 10.1103/PhysRevD.81.051501 PACS numbers: 13.85.Hd, 11.55.Bq

In this paper we expand our approach to soft hadron interactions, developed in Ref. [1], to obtain estimates for single inclusive cross sections. We have two main objectives: First, we wish to reproduce the existing data and predict the single inclusive experimental distributions which will be measured in the preliminary low-luminosity LHC runs. The data for $\sqrt{s} = 200$–1800 GeV are well reproduced by our model. The first published LHC experimental output [2], provides data on p-p single inclusive cross sections at $\sqrt{s} = 900$ GeV which is in accord with the results of our model. Second, the successful data analysis presented in this paper follows directly from the Gotsman-Levin-Maor-Miller (GLMM) model and its fitted parameters [1]. As such, it provides additional support to the validity of our hypothesis.

In our approach to soft Pomeron interactions we combine two elements: A two channel Good-Walker mechanism [3] with a supercritical Regge-like Pomeron with an intercept $\Delta_P > 0$, to which we add the enhanced (multi-)Pomeron interactions. Our formulation is based on two main assumptions:

(1) We assume that the slope of the Pomeron trajectory $\alpha'_P = 0$. This assumption is strongly supported by the global data analysis we have presented in Ref. [1], in which the fitted value of α'_P is exceedingly small. A consequence of the small value of α'_P is a relatively large $\Delta_P \simeq 0.35$.

(2) In our calculations of enhanced (and semienhanced) Pomeron interactions we only take into account the triple Pomeron vertex.

These assumptions are compatible with the main features of the Pomeron in $N = 4$ supersymmetric Yang-Mills theory, in which the Pomeron has an intercept of $\Delta_P = 1 - 2/\sqrt{\lambda}$ at large values of λ, and $\alpha'_P = 0$. Note that the fitted value $\Delta_P \simeq 0.35$ obtained in our model corresponds to a large value of $\lambda \simeq 10$. In this approach, the main contributions to the total cross section are the elastic and diffractive cross sections. This is a consequence of the Good-Walker mechanism [3] coupled to the vanishing of the cross sections initiated by multi-Pomeron interactions (for details see Ref. [1]). The strength of the Pomeron interaction is proportional to $2/\sqrt{\lambda}$, which can be taken into account by introducing a triple Pomeron vertex.

Our Pomeron model assumptions provide a natural matching between soft Pomeron dynamics and high density QCD (hdQCD); see Refs. [4–11]. The only hdQCD dimensional scale which is responsible for high energy interactions is Q_s, the saturation scale. This scale increases with energy leading to $\alpha'_P \propto 1/Q_s^2(x) \rightarrow 0$ at high enough energies where $x \rightarrow 0$. Recall that the triple Balitsky-Fadin-Kuraev-Lipatov Pomeron vertex plays a decisive role in small x perturbative QCD [6,9,10,12–17]. The consequent emerging compatibility of soft and hard Pomeron dynamics and their similar formulations are the main results of our Pomeron studies.

In the framework of Pomeron calculus [18] (see also Refs. [19–21]), single inclusive cross sections can be calculated using the Mueller diagrams [22] shown in Figure 1(a). They lead to

$$\begin{aligned}\frac{1}{\sigma_{\rm in}}\frac{d\sigma}{dy} = \frac{1}{\sigma_{\rm in}(Y)}\{&a_{PP}(\alpha^2 g_1 + \beta^2 g_2)^2 G_{\rm enh}(T(Y/2 - y))\\ &\times G_{\rm enh}(T(Y/2 + y)) - a_{RP}(\alpha^2 g_1^R + \beta^2 g_2^R)\\ &\times (\alpha^2 g_1 + \beta^2 g_2)\\ &\times [e^{(\Delta_R(Y/2-y)} \times G_{\rm enh}(T(Y/2+y))\\ &+ e^{(\Delta_R(Y/2-y)} \times G_{\rm enh}(T(Y/2+y))]\}, \qquad (1)\end{aligned}$$

where the Pomeron Green's function is

$$G_{\rm enh}(Y) = 1 - \exp\left(\frac{1}{T(Y)}\right)\frac{1}{T(Y)}\Gamma\left(0, \frac{1}{T(Y)}\right). \qquad (2)$$

Following Gribov [18], we take into account in Eq. (1) the sum of the Pomeron enhanced diagrams, considering them as a first approximation for the exact Green function of the Pomeron (Fig. 1(b)). Equation (2) gives the explicit form of

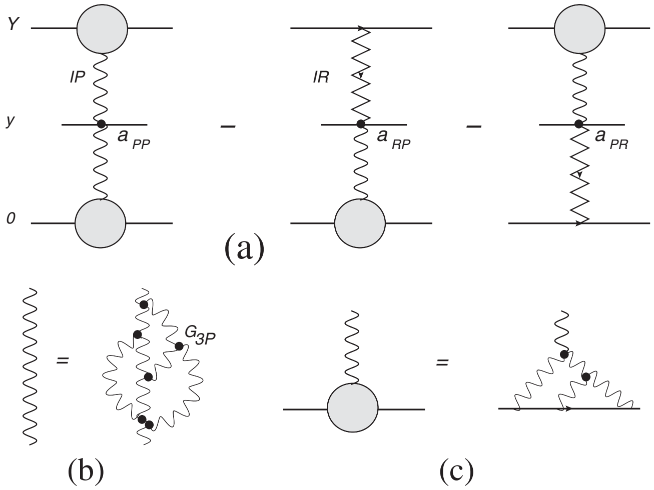

FIG. 1. Mueller diagrams [22] for a single inclusive cross section. A bold waving line presents the exact Pomeron Green function of (2), which is the sum of the enhanced diagrams of Fig. 1(b). A zigzag line corresponds to the exchange of a Reggeon.

this Green function for $\alpha'_P = 0$. Also included in Eq. (1) are the contributions of the secondary Reggeons.

In Eq. (1) we have introduced two new phenomenological parameters, a_{PP} and $a_{PR} = a_{RP}$, for the description of hadron emission from the Pomeron and Reggeon. There is an additional dimensional parameter, denoted by Q, which represents the average transverse momentum of the produced minijets. $Q_0 Q$ is the effective mass squared of these minijets, with $Q_0 = 2$ GeV (see Ref. [23] for details). Q and Q_0 are needed to calculate the pseudorapidity η which replaces the rapidity y. The relation between y and η is well known (see, for example, Ref. [23]),

$$y(\eta, Q) = \frac{1}{2}\ln\left\{\frac{\sqrt{\frac{Q_0 Q + Q^2}{Q^2} + \sinh^2\eta} + \sinh\eta}{\sqrt{\frac{Q_0 Q + Q^2}{Q^2} + \sinh^2\eta} - \sinh\eta}\right\}, \quad (3)$$

with the Jacobian

$$h(\eta, Q) = \frac{\cosh\eta}{\sqrt{\frac{Q_0 + Q}{Q} + \sinh^2\eta}}. \quad (4)$$

In the parametrization of Ref. [1], the value of the Pomeron-particle vertices are large. To compensate, we also sum the semienhanced diagrams which contribute to the exact vertex of the Pomeron-particle interaction (see Fig. 1(c)). This vertex is equal [24,25] to

$$G_{\rm enh}(y) g_i(b) \to g_i(b, y) = g_i G_{\rm enh}(y) S_i(b)/(1 + g_i G_{\rm enh}(y) S_i(b)), \quad (5)$$

where [1]

$$S_i(b) = \frac{m_i^2}{4\pi} b m_i K_1(m_i b). \quad (6)$$

Using Eq. (5), we obtain

$$\frac{1}{\sigma_{\rm in}}\frac{d\sigma}{dy} = \frac{1}{\sigma_{\rm in}(Y)}\Big\{a_{PP}\Big(\int d^2b(\alpha^2 g_1(b, Y/2 - y) + \beta^2 g_2(b, Y/2 - y)) \times \int d^2b(\alpha^2 g_1(b, Y/2 + y) + \beta^2 g_2(b, Y/2 + y)) - a_{RP}(\alpha^2 g_1^R + \beta^2 g_2^R)\Big(\alpha^2 \int d^2b(\alpha^2 g_1(b, Y/2 - y) + \beta^2 g_2(b, Y/2 - y))e^{\Delta_R(Y/2+y)} + \int d^2b(\alpha^2 g_1(b, Y/2 + y) + \beta^2 g_2(b, Y/2 + y))e^{\Delta_R(Y/2-y)}\Big)\Big\}. \quad (7)$$

Introducing a new notation,

$$V(y) = \int d^2b \tilde{V}(b, y) = \int d^2b(\alpha^2 g_1(b, Y/2 - y) + \beta^2 g_2(b, Y/2 - y)), \quad (8)$$

we obtain a more compact expression for Eq. (7)

$$\frac{1}{\sigma_{\rm in}}\frac{d\sigma}{dy} = \frac{1}{\sigma_{\rm in}(Y)}\{a_{PP}V(y/2 - y)V(Y/2 + y) - a_{RP}(\alpha^2 g_1^R + \beta^2 g_2^R)(V(Y/2 - y)e^{(\Delta_R(Y/2+y)} + V(Y/2 + y)e^{(\Delta_R(Y/2-y))}\}. \quad (9)$$

Equation (9) enables us to calculate the single inclusive density as a function of the pseudorapidity η.

As noted, this calculation entails three additional parameters. The determination of these parameters from existing data [26] is not trivial. Comparing the numbers corresponding to the data shown in Fig. 2, it is evident that a conventional overall χ^2 analysis is impractical, owing to the quoted error bars of the 546 GeV data points, which are considerably smaller than the error bars quoted for the other energies. The full lines in Fig. 2 are the results derived from a χ^2 fit to the 200–1800 GeV data, excluding the 546 GeV points. This fit yields a seemingly poor

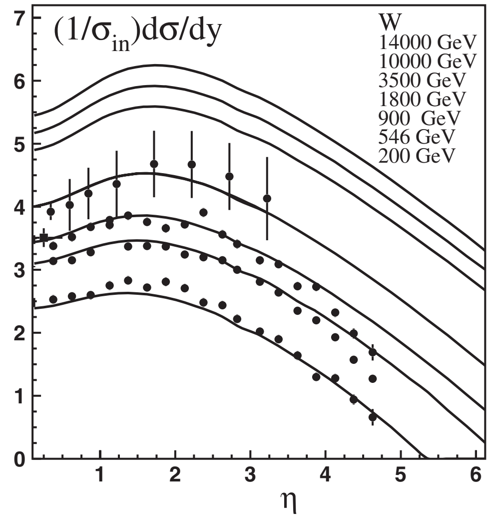

FIG. 2. Single inclusive density versus energy. The dotted data were taken from Ref. [26]. The square data point corresponds to the first experimental data from LHC by the Alice Collaboration [2].

$\chi^2/\mathrm{DOF} = 3.2$. Despite this, we consider this fit to be acceptable, as the data points ''oscillate'' about a uniform line with error bars which are much smaller than their deviation from a smooth average. The results of this fit are $a_{PP} = 75.7$, $a_{PR} = 0.12$, and $Q = 3.8$ GeV. In our procedure, the line for 546 GeV in Fig. 2 is calculated with the model parameters and is visually compatible with the experimental data points. Note that both the axes of Fig. 2 are linear, and that our calculation coincides with the first LHC experimental result [2]. We have also made predictions for the higher energies at which the LHC is expected to run; see Fig. 2. The contributions of the secondary Regge trajectories are minimal. The experimental values for $\sigma_{\rm in} = \sigma_{\rm tot} - \sigma_{\rm el} - \sigma_{\rm diff}$ were taken from Refs. [2,26]. For our predictions we have used the values of $\sigma_{\rm in}$ calculated in our GLMM model. Our output overestimates the few data points with $\eta > 4$ data at 546 and 900 GeV by up to 20%. This is to be expected, as we have not taken into account the parton correlations due to energy conservation, which are important in the fragmentation region, but difficult to include in the framework of Pomeron calculus.

To summarize, we have presented a theoretical formulation for single inclusive hadron-hadron interactions based on our GLMM model. We have reproduced the p-p data [2,26] on single inclusive density as a function of the pseudorapidity. Our results provide additional support for our proposed Pomeron approach. We have also presented predictions for the LHC energy range. These predictions may soon be tested during the preliminary low-luminosity LHC runs.

This research was supported in part by BSF Grant No. 20004019.

[1] E. Gotsman, E. Levin, U. Maor, and J. S. Miller, Eur. Phys. J. C **57**, 689 (2008); arXiv:0903.0247.
[2] ALICE Collaboration, Eur. Phys. J. C **65**, 111 (2010).
[3] M. L. Good and W. D. Walker, Phys. Rev. **120**, 1857 (1960).
[4] E. A. Kuraev, L. N. Lipatov, and F. S. Fadin, Zh. Eksp. Teor. Fiz. **72**, 377 (1977) [Sov. Phys. JETP **45**, 199 (1977)]; Ya. Ya. Balitsky and L. N. Lipatov, Yad. Fiz. **28**, 1597 (1978) [Sov. J. Nucl. Phys. **28**, 822 (1978)].
[5] L. N. Lipatov, Phys. Rep. **286**, 131 (1997); Zh. Eksp. Teor. Fiz. **90**, 1536 (1986), and references therein [Sov. Phys. JETP **63**, 904 (1986), and references therein].
[6] L. V. Gribov, E. M. Levin, and M. G. Ryskin, Phys. Rep. **100**, 1 (1983).
[7] A. H. Mueller and J. Qiu, Nucl. Phys. **B268**, 427 (1986).
[8] L. McLerran and R. Venugopalan, Phys. Rev. D **49**, 2233 (1994); **50**, 2225 (1994); **53**, 458 (1996); **59**, 094002 (1999).
[9] I. Balitsky, Nucl. Phys. **B463**, 99 (1996); Phys. Rev. D **60**, 014020 (1999).
[10] Y. V. Kovchegov, Phys. Rev. D **60**, 034008 (1999).
[11] J. Jalilian-Marian, A. Kovner, A. Leonidov, and H. Weigert, Phys. Rev. D **59**, 014014 (1998); Nucl. Phys. **B504**, 415 (1997); J. Jalilian-Marian, A. Kovner, and H. Weigert, Phys. Rev. D **59**, 014015 (1998); A. Kovner, J. G. Milhano, and H. Weigert, Phys. Rev. D **62**, 114005 (2000); E. Iancu, A. Leonidov, and L. D. McLerran, Phys. Lett. B **510**, 133 (2001); Nucl. Phys. **A692**, 583 (2001); E. Ferreiro, E. Iancu, A. Leonidov, and L. McLerran, Nucl. Phys. **A703**, 489 (2002); H. Weigert, Nucl. Phys. **A703**, 823 (2002).
[12] M. A. Braun, Phys. Lett. B **632**, 297 (2006); Eur. Phys. J. C **16**, 337 (2000); Phys. Lett. B **483**, 115 (2000); Eur. Phys. J. C **33**, 113 (2004); **6**, 343 (1999); M. A. Braun and G. P. Vacca, Phys. Lett. B **454**, 319 (1999).
[13] J. Bartels, M. Braun, and G. P. Vacca, Eur. Phys. J. C **40**, 419 (2005); J. Bartels and C. Ewerz, J. High Energy Phys. 09 (1999) 026; J. Bartels and M. Wusthoff, Z. Phys. C **66**, 157 (1995); A. H. Mueller and B. Patel, Nucl. Phys. **B425**, 471 (1994); J. Bartels, Z. Phys. C **60**, 471 (1993).
[14] A. H. Mueller, Nucl. Phys. **B415**, 373 (1994); **B437**, 107 (1995).
[15] E. Laenen and E. Levin, Nucl. Phys. **B451**, 207 (1995).
[16] E. Levin and M. Lublinsky, Nucl. Phys. **A763**, 172 (2005); Phys. Lett. B **607**, 131 (2005); Nucl. Phys. **A730**, 191 (2004).

[17] E. Levin, J. Miller, and A. Prygarin, Nucl. Phys. **A806**, 245 (2008).

[18] V. N. Gribov, Zh. Eksp. Teor. Fiz. **53**, 654 (1967) [Sov. Phys. JETP **26**, 414 (1968)].

[19] P. D. B. Collins, *An Introduction to Regge Theory and High Energy Physics* (Cambridge University Press, Cambridge, England, 1977).

[20] Luca Caneschi, *Regge Theory of Low-p_T Hadronic Interaction* (North-Holland, Amsterdam, 1989).

[21] E. Levin, arXiv:hep-ph/9808486; arXiv:hep-ph/9710546.

[22] A. H. Mueller, Phys. Rev. D **2**, 2963 (1970).

[23] D. Kharzeev and E. Levin, Phys. Lett. B **523**, 79 (2001).

[24] A. Schwimmer, Nucl. Phys. **B94**, 445 (1975).

[25] K. G. Boreskov, A. B. Kaidalov, V. A. Khoze, A. D. Martin, and M. G. Ryskin, Eur. Phys. J. C **44**, 523 (2005).

[26] C. Amsler *et al.* (Particle Data Group), Phys. Lett. B **667**, 1 (2008).